



Published in final edited form as:

*Adv Biomed Eng Res.* 2015 ; 3: 8–17. doi:10.14355/aber.2015.03.002.

## A Coaxial Dielectric Probe Technique for Distinguishing Tooth Enamel from Dental Resin

Paul M. Meaney<sup>1</sup>, Benjamin B. Williams<sup>2</sup>, Shireen D. Geimer<sup>2</sup>, Ann B. Flood<sup>2</sup>, and Harold M. Swartz<sup>2</sup>

<sup>1</sup> Thayer School of Engineering, Dartmouth College, Hanover, NH USA

<sup>2</sup> Geisel School of Medicine, Dartmouth College, Hanover, NH USA

### Abstract

For purposes of biodosimetry in the event of a large scale radiation disaster, one major and very promising point-of contact device is assessing dose using tooth enamel. This technique utilizes the capabilities of electron paramagnetic resonance to measure free radicals and other unpaired electron species, and the fact that the deposition of energy from ionizing radiation produces free radicals in most materials. An important stipulation for this strategy is that the measurements, need to be performed on a central incisor that is basically intact, i.e. which has an area of enamel surface that is as large as the probing tip of the resonator that is without decay or restorative care that replaces the enamel. Therefore, an important consideration is how to quickly assess whether the tooth has sufficient enamel to be measured for dose and whether there is resin present on the tooth being measured and to be able to characterize the amount of surface that is impacted. While there is a relatively small commercially available dielectric probe which could be used in this context, it has several disadvantages for the intended use. Therefore, a smaller, 1.19mm diameter 50 ohm, open-ended, coaxial dielectric probe has been developed as an alternative. The performance of the custom probe was validated against measurement results of known standards. Measurements were taken of multiple teeth enamel and dental resin samples using both probes. While the probe contact with the teeth samples was imperfect and added to measurement variability, the inherent dielectric contrast between the enamel and resin was sufficient that the probe measurements could be used as a robust means of distinguishing the two material types. The smaller diameter probe produced markedly more definitive results in terms of distinguishing the two materials.

### Keywords

Dielectric Properties; Tooth Enamel; Dental Resin; Electron Paramagnetic Resonance; Open-Ended Coaxial Probe; Radiation Dosimetry

---

Correspondence to: Paul M. Meaney.

paul.meaney@dartmouth.edu; benjamin.b.williams@dartmouth.edu; shireen.d.geimer@dartmouth.edu

## Introduction

Electron paramagnetic resonance (EPR) measurements made in vivo using the enamel in incisors are being developed as a biodosimetric method capable of quickly assessing whether a person has received a clinically significant radiation dose after a large-scale radiation accident or explosion [1]. In planning scenarios from the US federal government, up to a million people could be potentially exposed in such an event and those at risk for suffering from acute radiation syndrome (ARS) need to receive life-saving medical care within hours to days following the event [2-7]. The health care system would be immediately overwhelmed by such numbers and so the emergency medical response system needs to quickly assess each victim's dose to be able to appropriately triage into medical care for those who are at risk for ARS and triage out of the medical care system for those who could not benefit from acute care [4-6]. Because this initial triage is intended to keep people away from the health care system, federal disaster planners have argued that it is important that the biodosimetry methods used have a low false negative rate, i.e., no one who is turned away from the medical care system should in fact need immediate life-saving care [3].

There are several biodosimetric methods under development to carry out this initial triage. One which is especially well suited for rapid, point-of-care triage is in vivo EPR tooth dosimetry [8-11]. The free radicals generated in teeth by ionizing radiation are very stable and not subject to variation by variations in individuals due to chronic or acute stress or disease and therefore act as excellent passive dosimeters [10]. The EPR technique is able to precisely measure the number of free radicals present and provide accurate renderings of the associated dose [12].

Dose assessment based on EPR tooth dosimetry could be impacted by the amount of enamel –or by the misidentification of artificial applications from restorative dentistry as ‘true’ enamel. Consequently, it is important to quickly assess whether the surface of the tooth being queried by EPR is in fact mostly or entirely enamel. This assessment is rendered difficultly in many cases, particularly on the front teeth, because dentistry has successfully developed ways to make these restorations very difficult to discern from natural enamel in teeth.

Mistaking resin for enamel could likely to lead to false negative measurements in people who were in fact exposed to dose, because the resin does not respond to radiation [13]. As noted above, avoiding false negatives is important for initial triage. Therefore, it is critical to devise a simple strategy for determining whether the tooth surface under examination contains any resin or other artificial surface. While people could be asked to report whether their teeth have a filling or artificial cap, in practice many people actually cannot remember which tooth had had restorative dentistry, so a simple patient survey is not sufficiently reliable.

Dielectric property measurements have been studied and exploited for numerous applications over multiple decades. Some of the more recent research has been done in biomedical applications where scientists have assessed the behavior of tissue dielectric

properties and how they might be used in screening, diagnosis and treatment monitoring. Gabriel et al [14-16] performed a thorough study of a variety of tissue types over a broad frequency range to establish useful baselines. Some of the more notable applications have been done in monitoring temperature during thermal therapy by imaging the dielectric property changes [17,18]. Schnabel et al [19] has developed a coaxial dielectric probe technique for measuring the surface properties of excised breast tissue for determining whether the surgical margins are sufficiently based on the endogenous dielectric property contrast between normal and malignant tissue. Also in the breast tissue setting, several groups have developed techniques for imaging the breast and either detecting or diagnosing tumors with respect to the tumor: benign property contrast [20,21].

The most common way of assessing dielectric properties is the open ended coaxial probe. These have been studied at length and are used regularly in commercial and scientific laboratories [14-16]. One of the more recent assumptions has been that these types of probes provide average bulk measures of the properties to a depth of several millimeters [22]. This has had important implications for investigating heterogeneous tissues such as the breast [23]. However, it has been recently demonstrated that these assumptions were incorrect and that the effective depth of penetration for the open-ended coaxial probes was actually quite shallow – on the order of 0.3mm - for commercially available probes [24] and that it was also a function of the probe diameter [25]. While this result raises questions about the conclusions of the afore-mentioned breast tissue property study, it opens up new possibilities for this style probe. In particular, with their penetration depth being so shallow, these types of probes are ideally suited for superficial measurements. In this case, testing tooth enamel is an intriguing application because of the generally thin layer of enamel covering the underlying dental anatomy.

While the open-ended coaxial probe has gained widespread acceptance, two notable characteristics limit its use. First, as noted above, the effective depth of penetration for probes is dependent on the coaxial opening diameter and is generally only a fraction of a millimeter deep for the most practical probe sizes [26,27]. Delfin Technologies has developed a suite of varying diameter probes for measuring the level of edema at different depths [28]. These probes range from 10 to 55 mm diameter with a maximum penetration depth of 5.0 mm. An equally confounding issue is the level to which the probes require intimate contact with the target. For instance, manufacturers generally recommend against using coaxial probes for solid surfaces because it is difficult to make full contact with the inner conductor and the full circumference of the outer conductor [24]. These probes effectively generate a weighted average measurement for the sampling zone within the first 10ths of a millimeter from its surface. In the event that air is part of that mixture, whose effect can be considerable because air's properties are so low compared to most tissue types. With an imperfect contact, the proportion of air in the sampling zone can vary and substantially distort the desired measurement.

In the tooth measurement scenario, we exploit these characteristics such that the probe can be used as a technique for distinguishing natural tooth enamel from common dental resins. First, the thin layers of the enamel and resin are ideal targets for a small probe because of the associated shallow penetration depths. The tooth is a remarkably complex and

heterogeneous tissue containing enamel, dentin, pulp, etc., with each component presenting different dielectric properties. The enamel typically ranges between 0.3 and 1.0 mm on the nominally outer flat surface of an incisor, so a probe with a substantially deeper penetration depth would also incorporate properties from the underlying dentin and such into the bulk property measurements. Using a small probe isolates the measurements right at the surface. In addition, a smaller probe diameter directly implies that the amount of intervening air between the probe and tooth is reduced for a fixed radius of curvature. While the measurements on a non-flat surface will inherently contain property contributions from the intervening air, if the air portion is minimized and there is sufficient dielectric property contrast between the resin and enamel, it is possible to utilize a small diameter probe for this application. Additional practical constraints come from the intended use, which includes being used near a disaster site where there are likely to be limitations in availability of power, expertise, and time to make the measurement. Ideally the probe should be robust, very portable, and able to be used by a non-expert. It could be advantageous to be able to make it a part of the dosimetry device.

While the probe interface is an essential consideration for applying this technology, the associated vector network analyzer (VNA) required for the measurements has been a considerable limitation in preventing more widespread use [29,30]. The conventional VNA is large and cumbersome and quite expensive. In recent years handheld units and systems with significantly reduced profiles have become commercially available but are still expensive [31-32]. However, even these revolutions are minor compared with system-on-a-chip advances that are making it possible to produce VNA's on a chip [33-37]. While these are not yet commercially available at the chip level, they are nonetheless being used in current generation network analyzers [38]. Given the pace of innovation and development in the semiconductor world, it is natural to expect these devices to be available at the chip level in coming years. This has the potential to radically open up windows for dielectric property measurements in an array of commercial and clinical applications.

The Methods section describes the probes used, the dielectric property measurement set-up and a comparison of the air contribution for two different diameter probes. The Results section provides a validation study of the specialized, small diameter probes for several known liquid standards and a comparison of dielectric property measurements for two different probes on a number of repeated scans on representative teeth enamel and dental resins, respectively. The preliminary results indicate that when the probe diameter is sufficiently small, the dielectric measurements are capable of distinguishing enamel from resin surfaces to a statistically significant level.

## Methods

### Open-Ended Coaxial Dielectric Probe Measurements

Two open-ended coaxial probes were used in this experiment (Fig. 1). The first is the standard Slim Form probe produced by Agilent Technologies (Santa Clara, CA). It is constructed from a standard length of 2.16mm diameter semi-rigid coaxial cable (RG-405) having center conductor and insulator diameters of 0.51mm and 1.68mm, respectively. For most of the cable length the insulator is Teflon; however, for the short distance nearest the

open-ended probe, the Teflon has been replaced with a borosilicate glass bead to form a more hermetic seal and eliminate possible wicking of liquids-under-test into the spaces between the conductors and insulator [39]. The custom probe is fabricated from a 1.19mm diameter length of semi-rigid coaxial cable with the surface ground flat. The center conductor and insulator diameters were 0.28mm and 0.94mm, respectively, and the insulator was made from Teflon.

The dielectric properties of an unknown sample are computed directly from the S11 measurements with the reference plane set exactly at the probe interface. The calibration utilized three references: open circuit (air), short circuit, and water (25°C). For the short circuit, a thin film of aluminum foil was pressed up against the probe with a flexible piece of flat rubber behind it to ensure accurate electrical contact between the conductors and the shorting material. The algorithm is comparable to the gradient-descent method with first order differentiation developed by Grant et al [40]. In this situation, we utilized the commercial software package from the Agilent Dielectric Probe Kit (85070E) with both probes. While the software package is specifically designed with the dimensions of the larger probe in mind, as shown in the Results section, the differences when applying the algorithm across two different diameter probes is inconsequential for this application.

### Probe Penetration Depth

Previous reports have demonstrated correlation with probe diameter size and penetration depth [22,23]. In fact, Delfin Technologies produces a suite of varying diameter dielectric probes for different penetration depths for monitoring edema (Table 1) [28].

In addition to this analysis, the penetration depth for the Agilent probe was computed to be 0.28mm [25]. By extrapolating these data points, the penetration depth for the 1.19mm diameter coaxial probe was estimated to be on the order of 0.17mm. While the thickness of the enamel varies depending on the position on the tooth, for most fairly flat surfaces the values are nominally between 0.3 and 1.0mm allowing the probe measurements to reliably interrogate primarily just the enamel and resin.

### Impact of Air on the Sensing Volume

In Meaney et al [25], the interpretation of the penetration depth is that for a multi-layered target, for which the recovered properties are very nearly a weighted average of the fractional volume of the different property components. In this case, because air has such a proportionally large difference in properties with respect to both enamel and resin, it is critical to assess the proportion of air in the associated sensing volumes. Fig. 2 shows a schematic diagram of the probe sensing volume and the enamel surface modeled as a spherical surface with a defined radius of curvature.

In this case,  $t$  is the penetration depth for a given probe and  $T$  is the layer thickness that partially includes air (for calculation simplicity, we assume that the probe contacts the curved zone directly in the center and the surface of the tooth is a perfect sphere). For this configuration, the radius of curvature is  $r$  and the radius of the particular probe is  $h$ . In this case, the total sensing volume is defined as:

$$V_t = \pi h^2 t \quad (1)$$

And the volume of the air is that portion of the sensing volume cylinder that intersects the edge of the tooth ( $V_T$ ) minus the curved zone of the tooth within that cylinder:

$$V_{air} = V_T - V_{curved \ zone} = \pi h^2 T - V_{curved \ zone} \quad (2)$$

In this case, the volume of the curved zone is equal to the spherical sector volume with a specific radius and enclosed angle,  $\alpha$ , minus the volume of a circular cone where the flat surface corresponds to the plane defined where sensing volume cylinder contacts the tooth surface

$$V_{curved \ zone} = V_{spherical \ sector} - V_{circular \ cone} = \frac{2\pi r^2 T}{3} - \frac{2\pi h^2 (r - T)}{3} \quad (3)$$

Overall the percent contribution of air to the sensing volume is

$$\frac{V_T - (V_{spherical \ sector} - V_{circular \ cone})}{V_t} * 100\% \quad (4)$$

### In Vitro Tooth Measurements

For these experiments we used cadaver teeth that had been stored at 4°C. Purely enamel and resin coated surfaces were identified by a dentist. Fig. 3 shows photographs of representative measurements using both probes. In all cases the probes were calibrated while held stationary in the probe stand. For each measurement, one technician manually held the end of the probe up against the tooth surface while the other controlled the software and network analyzer. This technique is representative of the challenges of using this type of device in an actual clinical setting.

## Results

### Validation of Dielectric Probe Measurements

Fig. 4a and b show the measured dielectric properties of three standards (water, methanol, and ethanol) from 0.1 to 8.5 GHz using both the large and small probes, respectively. In all cases, three sets of data were taken and averaged for each curve. Error bars and/or confidence intervals are not shown because they are so small and would disrupt the main emphasis of the results. For the larger probe, the relative errors were under 0.5% and 0.7% for the permittivity and conductivity, respectively. For the smaller probe, the relative errors were under 0.4% and 0.5% for the permittivity and conductivity, respectively. Overall the agreement between the two probes is quite good. For the permittivity the maximum relative error is roughly 10% while the values for the conductivity are lowest at the lower frequencies and increase monotonically up to 19% for the worst case of the higher frequencies. The conductivity errors are also highest for the ethanol and methanol where the

nominal values are considerably lower than those for water. The error values for the water are somewhat artificially low since water is also used as a calibration standard.

### Radius of Curvature Analysis

Using the analysis developed in Section II.C, we plot the percentage of air in the sensing volume for each probe as a function of the ideal tooth radius of curvature (Fig. 5).

Given that the effective bulk dielectric measurement roughly approximates a weighted average of the volume fractions of the constituent dielectric properties, the percentage air is a large confounder for the desired permittivity and conductivity. In both cases, the percentage of air increases rapidly as the radius of curvature decreases which implies that measurements near and around tooth edges would be more vulnerable to corruption from air contributions. The air percentages are also consistently less for the smaller diameter probe which makes intuitive sense in that as the probe size nears a single point, the contact on a curved surface would approach a perfect contact. Our experience with the clinical EPR measurements is that the teeth surfaces for the flattest sections of the incisors have radii of curvature near 15 mm. This indicates that the percent air contributions for the large and small probe would roughly be 4.7 and 2.9%, respectively.

### Comparison of Large and Small Probe Data

For this experiment, we measured five different teeth which were either entirely enamel covered or had a hybrid of enamel and resin on the surface. The teeth designations first indicate which tooth is selected (T8 is the patient's right upper incisor and T9 is the left upper incisor), the second number is the patient index and finally it is noted whether the test location was for enamel or resin. The seven designations were: T8-52 enamel, T8-79 enamel, T8-143 enamel, T9-67 enamel, T9-131 enamel, T8-52 resin, and T9-131 resin. For each set we took between 2 and 6 measurements for a total of 27 measurements with each probe. Fig. 6 shows two graphs summarizing the measured relative permittivity data as a function of frequency for the small probe (note that the conductivity values are quite low for both and the inherent values are most likely indistinguishable between those for the enamel and resin). Fig. 6a shows the permittivity values for all measurements as a function of frequency for all enamel and resin measurements. The blue curves are for the enamel samples and the red for the resin with the heavier black lines designating the averages of each. In this case the average enamel values range roughly from 2.4 to 4.6 with an average of 4.0 and from roughly 2.2 to 2.7 with an average of 2.5 for the resin. There is almost no overlap between values and the two sets appear reasonably distinguishable from each other. Fig. 6b shows the average data for each tooth plotted as a function of frequency. In this case there is no overlap at all between the enamel and resin sets.

Fig. 7 shows two graphs summarizing the measured data as a function of frequency for the large probe. In this case the values for the enamel and resin measurements vary widely. The enamel values range as high as 6.0 and as low as 1.0. Those for the resin range from 1.2 to about 4.2. The averages still show a difference between the two sets; however there is considerable overlap between individual measurements. The averages for the individual teeth (Fig. 7b) also confirm this trend.



## Discussion and Conclusions

The new smaller probe has been shown to be equally accurate in determining the dielectric properties in reference liquids. With respect to actual tooth measurements, both sets of scans confirm that there is an inherent contrast in properties between the enamel and resin. However, the probe contact can have a significant impact on the measurement. It is clear that the smaller probe did a substantially better job in discriminating between enamel and resin than the larger one. This is most likely because it is inherently easier to minimize the contribution of air which is the primary confounder when the probe contact against solid material is imperfect.

It appears that the air contributions presented in Section III.B may understate the influence of the imperfect contact on the measurements. In addition, the poor contact most likely doesn't fully explain the erratic measurement behavior as a function of frequency or the wide variability within each class. It should be noted that the insulating material at the end of the smaller probe is Teflon which is quite malleable while that for the Agilent Slim Form probe is the more rigid borosilicate glass. It is possible that the Teflon is more capable of deforming slightly during the measurements and facilitating tighter contact with the tooth surface even under more challenging situations such as these.

The results appear promising – especially those for the smaller probe - and indicate that developing a more consistent means of contacting the probe would improve the overall consistency. The smaller probe has the desired characteristics of low power requirements and ease of use. Further developments are needed to assure sufficient robustness under field conditions. The full development of such a probe could be a significant advance in helping to determine which teeth are good EPR measurement candidates and improve the emergency screening process.

## ACKNOWLEDGMENT

This work was sponsored by Biomedical Advanced Research and Development Authority # HHSO100201100024C and NIH Grant # RO1-CA191227-01.

## REFERENCES

- [1]. Williams BB, Dong R, Flood AB, Grinberg O, Kmiec M, Lesniewski PN, Matthews TP, Nicolalde RJ, Raynolds T, Salikhov I, Swartz HM. A deployable in vivo EPR tooth Dosimeter for triage after a radiation event involving large populations. *Radiation Measurements*. 2011; 46:772–777. [PubMed: 21966241]
- [2]. National Security Staff. Interagency Policy Coordination Subcommittee for Preparedness and Response to Radiological and Nuclear Events. 2010. Planning Guidance for Reaction to a Nuclear Detonation. 2nd [http://hps.org/homeland/documents/Planning\\_Guidance\\_for\\_Response\\_to\\_a\\_Nuclear\\_Detonation-2nd\\_Edition\\_FINAL.pdf](http://hps.org/homeland/documents/Planning_Guidance_for_Response_to_a_Nuclear_Detonation-2nd_Edition_FINAL.pdf) [http://hps.org/homeland/documents/Planning\\_Guidance\\_for\\_Response\\_to\\_a\\_Nuclear\\_Detonation-2nd\\_Edition\\_FINAL.pdf](http://hps.org/homeland/documents/Planning_Guidance_for_Response_to_a_Nuclear_Detonation-2nd_Edition_FINAL.pdf) Accessed September 10, 2014
- [3]. Grace MB, Moyer BR, Prasher J, Cliffer KD, Ramakrishnan N, Kaminski J, Coleman CN, Manning RG, Maidment BW, Hatchett R. Rapid radiation dose assessment for radiological public health emergencies: Roles of NIAID and BARDA. *Health Physics*. 2010; 98:172–178. [PubMed: 20065680]



- [4]. DiCarlo AL, Maher C, Hick JL, Hanfling D, Dainiak N, Chao N, Bader JL, Coleman CN, Weinstock DM. Radiation injury after a nuclear detonation: medical consequences and the need for scarce resources allocation. *Disaster Medicine and Public Health Preparedness*. 2011; 5:S32–S44. [PubMed: 21402810]
- [5]. Coleman CN, Weinstock DM, Casagrande R, Hick JL, Bader JL, Chang F, Nemhauser JB, Knebel AR. Triage and treatment tools for use in a scarce resources-crisis standards of care setting after a nuclear detonation. *Disaster Medicine and Public Health Preparedness*. 2011; 5:S111–S121. [PubMed: 21402803]
- [6]. Knebel AR, Coleman CN, Cliffer KD, Murrain-Hill PM, McNally R, Oancea V, Jacobs J, Buddemeier B, Hick JL, Weinstock DM. Allocation of scarce resources after a nuclear detonation: setting the context. *Disaster Medicine and Public Health Preparedness*. 2011; 5:S20–S31. [PubMed: 21402809]
- [7]. AFRRRI (Armed Forces Radiobiology Research Institute). Medical Management of Radiological Casualties. 2010. Online Third Edition. <http://www.afrrri.usuhs.mil/outreach/infoprod.htm#guide> Accessed September 12, 2014
- [8]. Swartz HM, Flood AB, Williams BB, Meineke V, Dörr H. Comparison of the needs for biodosimetry for large-scale radiation events for military versus civilian populations. *Health Physics*. 2014; 106:755–763. [PubMed: 24776910]
- [9]. Swartz, HM.; Flood, AB.; Williams, BB.; Nicolalde, RJ.; Shapiro, A. Overview of Methods for Establishing Dose to Individuals for Managing Unplanned, Clinically Significant Exposures to Ionizing Radiation. In: Christensen, Doran M.; Sugarman, Stephen L.; O'Hara, Frederick M., Jr., editors. *The Medical Basis for Radiation-Accident Preparedness: Medical Management*. Oak Ridge Associated Universities; Oak Ridge, TN: 2014. p. 91-108.
- [10]. Iwasaki A, Grinberg O, Walczak T, Swartz HM. In vivo Measurements of EPR Signals in Whole Human Teeth. *Applied Radiation and Isotopes*. 2005; 62:187–190. [PubMed: 15607446]
- [11]. Brady JM, Aarestad NO, Swartz HM. In Vivo Dosimetry by Electron Spin Resonance Spectroscopy. *Health Physics*. 1968; 15:43–47. [PubMed: 4317533]
- [12]. Swartz HM, Williams BB, Flood AB. Overview of the principles and practice of biodosimetry. *Radiation and Environmental Biophysics*. 2014; 53:221–232. [PubMed: 24519326]
- [13]. Levêque P, Desmet C, Dos Santos-Goncalvez AM, Beun S, Leprince JG, Leloup G, Gallez B. Influence of Free Radicals Signal from dental resins on the Radio-Induced Signal in Teeth in EPR Retrospective Dosimetry. *PLOS ONE*. 2013; 8:e62225. [PubMed: 23704875]
- [14]. Gabriel C, Gabriel S, Corthout E. The dielectric properties of biological tissues: I. Literature survey. *Phys. Med. Biol.* 1996; 41:2231–2249. [PubMed: 8938024]
- [15]. Gabriel S, Lau RW, Gabriel C. The dielectric properties of biological tissues: II. Measurements on the frequency range 10 Hz to 20 GHz. *Phys. Med. Biol.* 1996; 41:2251–2269. [PubMed: 8938025]
- [16]. Gabriel S, Lau RW, Gabriel C. The dielectric properties of biological tissues: III. Parametric models for the dielectric spectrum of tissues. *Phys. Med. Biol.* 1996; 41:2271–2293. [PubMed: 8938026]
- [17]. Meaney PM, Paulsen KD, Fanning MW, Li D, Fang Q. Image accuracy improvements in microwave tomographic thermometry: phantom experience. *International Journal of Hyperthermia*. 2003; 19:534–550. [PubMed: 12944168]
- [18]. Meaney PM, Fanning MW, Paulsen KD, Li D, Pendergrass SA, Fang Q, Moodie KL. Microwave thermal imaging: Initial in vivo experience with a single heating zone. *International Journal of Hyperthermia*. 2003; 19:617–641. [PubMed: 14756452]
- [19]. Schnabel F, Susan K, Boolbol DM, Gittleman M, Karni T, Taфра L, Feldman S, Police A, Friedman NB, Karlan S, Holmes D, Willey SC, Carmon M, Fernandez K, Akbari S, Harness J, Guerra L, Frazier T, Lane K, Simmons RM, Estabrook A, Allweis T. A randomized prospective study of lumpectomy margin assessment with use of MarginProbe in patients with nonpalpable breast malignancies. *Annals of Surgical Oncology*. 2014; 21:1589–1595. [PubMed: 24595800]
- [20]. Poplack SP, Paulsen KD, Hartov A, Meaney PM, Pogue B, Tosteson T, Grove M, Soho S, Wells W. Electromagnetic breast imaging: pilot results in women with abnormal mammography. *Radiology*. 2007; 243:350–359. [PubMed: 17400760]

- [21]. Klemm, M.; Craddock, I.; Leendertz, J.; Preece, A.; Benjamin, R. IEEE AP-S; San Diego: Jul. 2008 Experimental and clinical results of breast cancer detection using UWB microwave radar; p. 5-11.1-4
- [22]. Hagl DM, Popovic D, Hagness SC, Booske JH, Okoniewski M. Sensing volume of open-ended coaxial probes for dielectric characterization of breast tissue at microwave frequencies, ". IEEE Transactions on Microwave Theory and Techniques. 2003; 51:1194–1206.
- [23]. Lazebnik M, Popovic D, McCartney L, Watkins CB, Lindstrom MJ, Harter J, Sewall S, Ogilvie T, Magliocco A, Breslin TM, Temple W, Mew D, Booske JH, Okoniewski M, Hagness SC. A large-scale study of the ultrawideband microwave dielectric properties of normal, benign and malignant breast tissues obtained from cancer surgeries. *Physics in Medicine and Biology*. 2007; 52:6093–6115. [PubMed: 17921574]
- [24]. Keysight Technologies. Dielectric probe kit 200 MHz to 50 GHz. Keysight Technologies, Inc.; Santa Clara, CA: 2014. Application Note: 5989-0222EN
- [25]. Meaney PM, Gregory A, Epstein N, Paulsen KD. Microwave open-ended coaxial dielectric probe: interpretation of the sensing volume re-visited. *BMC Medical Physics*. 2014; 14:1756–6649. paper #.
- [26]. Alanen E, Lahtinen T, Nuutinen J. Variational formulation of open-ended coaxial line in contact with layered biological medium. *IEEE Transactions on Biomedical Engineering*. 1998; 45:1241–1248. [PubMed: 9775538]
- [27]. Kiiskinen M, Nuutinen J, Alanen E. Measurement depths of a skin-water analyzer (MoistureMeter D). *Skin Research and Technology*. 2005; 11:292.
- [28]. Delfin Technologies, MoistureMeterD. [http://www.delfintech.com/en/moisturemeter\\_d/http://www.delfintech.com/en/moisturemeter\\_d/](http://www.delfintech.com/en/moisturemeter_d/http://www.delfintech.com/en/moisturemeter_d/)
- [29]. Agilent Technologies. Network analyzer basics. Agilent Technologies, Inc.; Santa Clara, CA: 2004. Application Note: 5965-7917E
- [30]. Agilent Technologies. E5071C ENA Network Analyzer. Agilent Technologies, Inc.; Santa Clara, CA: 2014. Application Note: 5989-5479EN
- [31]. Keysight Technologies. N9923A FieldFox RF Vector Network Analyzer. Keysight Technologies, Inc.; Santa Clara, CA: 2014. Application Note: 5990-5363EN
- [32]. Keysight Technologies. PXI Vector Network Analyzer Series. Keysight Technologies, Inc.; Santa Clara, CA: 2014. Application Note: 5992-0098EN
- [33]. Sutono A, Heo D, Chen E, Lim K, Laskar J. High Q LTCC-based passive library for wireless system-on-package (SOP) module development. *IEEE Transactions on Microwave Theory and Techniques*. 2001; 49:1715–1724.
- [34]. Lim K, Pintel S, Davis M, Sutono A, Lee C-H, Heo D, Abatoyabo A, Laskar J, Tantzzeris EM, Tummala R. RF-system-on-package (SOP) for wireless communications. *IEEE Microwave Magazine*. 2002:88–99.
- [35]. Laskar, J. System on package and system on chip trade-offs. presented at the IEEE Workshop on Circuits and Systems for Wireless Communications and Networking; South Bend, IN: Aug. 2001
- [36]. Azarian, MM. Vector network analyzer (VNA) on a chip. US Patent Publication; 2010. #US20100102829 A1
- [37]. Azarian, MM. Vector network analyzer (VNA) on a chip. US Patent Publication; 2013. #8378693 B2
- [38]. Anritsu Company. Compact Vector Network Analyzer. Anritsu Company; Richardson, TX: 2015. Application Note: 11410-00822B
- [39]. Blackham D, Pollard R. Finite element analysis of open-ended coaxial lines. *IEEE MTT-S*. 1993:1247–1250.
- [40]. Grant JP, Clarke RN, Symm GT, Spyrou NM. A critical study of the open-ended coaxial line sensor technique for RF and microwave complex permittivity measurements. *J Phys E Sci Instrum*. 1989; 22:757–770.

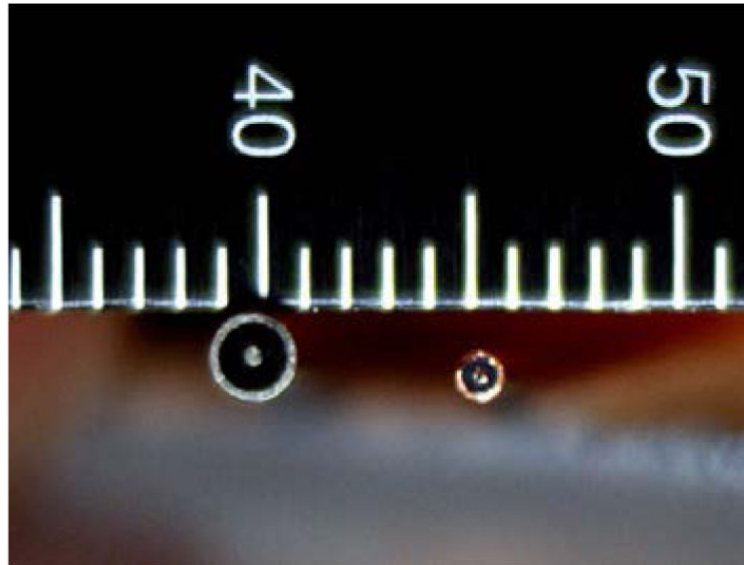


**FIGURE 1.** PHOTOGRAPH OF THE END OF THE TWO OPEN-ENDED COAXIAL PROBES: (LEFT) 2.16 MM DIAMETER SLIM FORM PROBE FROM AGILENT TECHNOLOGIES, AND (RIGHT) CUSTOM 1.19 MM DIAMETER SEMI-RIGID COAXIAL PROBE.

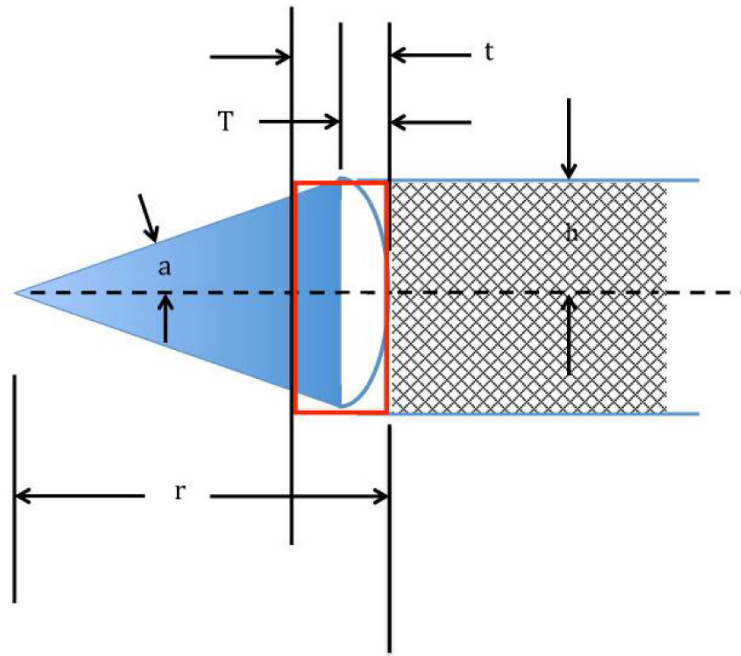


**FIGURE 2.** SCHEMATIC DIAGRAM SHOWING THE PROBE UP AGAINST THE CURVED TOOTH SURFACE, THE AIR GAPS BENEATH THE PROBE, THE PROBE SENSING VOLUME AND THE SPHERICAL SECTOR DEFINING THE RADIUS OF CURVATURE. DIMENSIONS INCLUDE:  $R$  – THE RADIUS OF CURVATURE,  $H$  – THE RADIUS OF THE COAXIAL PROBE,  $A$  – HALF OF THE SPHERICAL SECTOR ANGLE,  $T$  – THE HEIGHT OF THE PROBE SENSING VOLUME, AND  $T$  – THE HEIGHT OF THE CYLINDRICAL VOLUME FROM THE PROBE SURFACE TO WHERE AN IMAGINARY EXTENSION OF THE CYLINDER INTERSECTS THE TOOTH SURFACE.

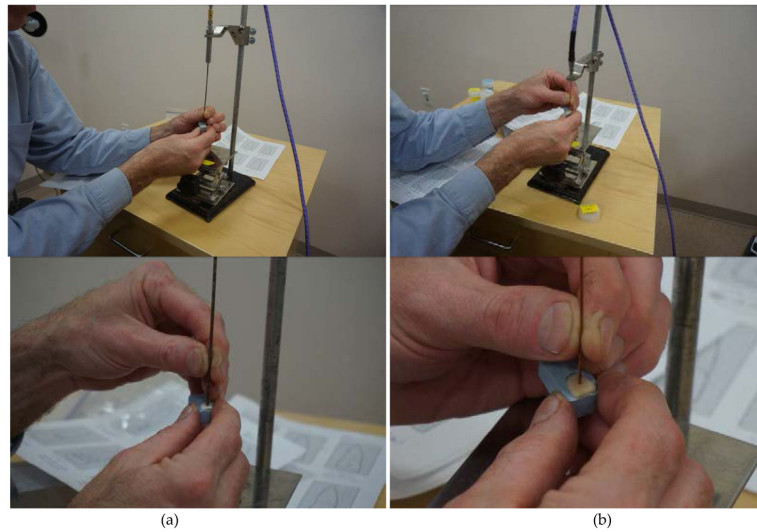


**FIGURE 3.** PHOTOGRAPHS OF THE (A) 2.16 MM DIAMETER SLIM FORM PROBE AND THE (B) 1.19MM DIAMETER COAXIAL PROBE BEING USED TO MEASURE THE DIELECTRIC PROPERTIES OF THE ENAMEL OF A TOOTH. THE FIELDS OF VIEW FOR THE TOP ROW PHOTOS SHOW THE COMPLETE STAND SET-UP WHILE THE BOTTOM ROW SHOWS CLOSE-UPS OF THE PROBE ACTUALLY CONTACTING THE TEETH.

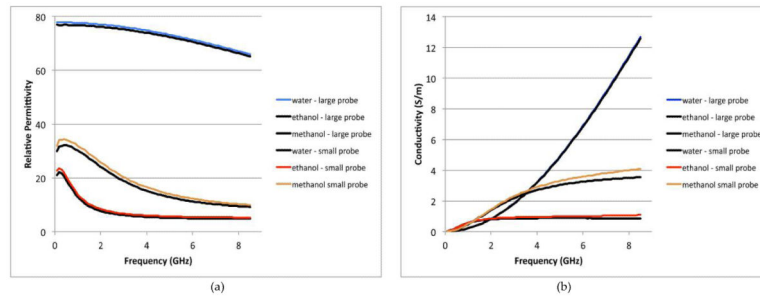


**FIGURE 4.** (A) RELATIVE PERMITTIVITY AND (B) CONDUCTIVITY MEASUREMENTS OF WATER, METHANOL, AND ETHANOL USING THE 2.16 MM DIAMETER SLIM FORM AND 1.19 MM DIAMETER PROBES, RESPECTIVELY.

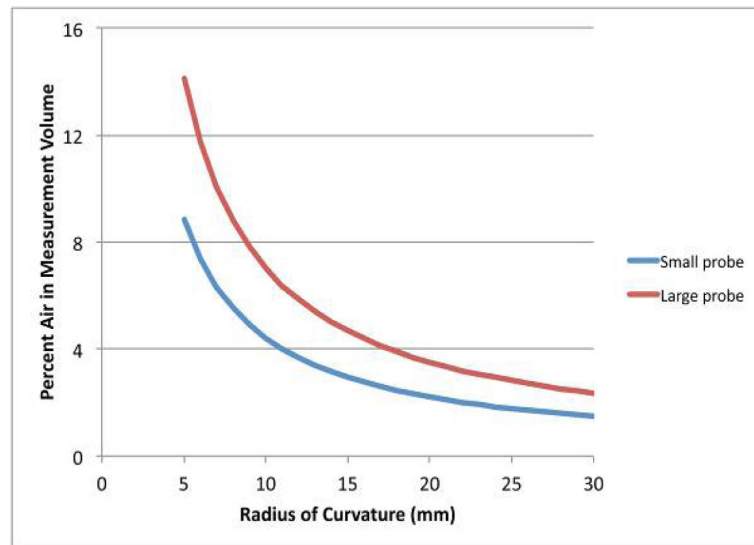


**FIGURE 5.** PLOTS OF THE PERCENTAGE OF AIR IN THE SENSING VOLUME AS A FUNCTION OF THE TOOTH RADIUS OF CURVATURE FOR BOTH THE 1.19 AND 2.16 MM DIAMETER PROBES, RESPECTIVELY.



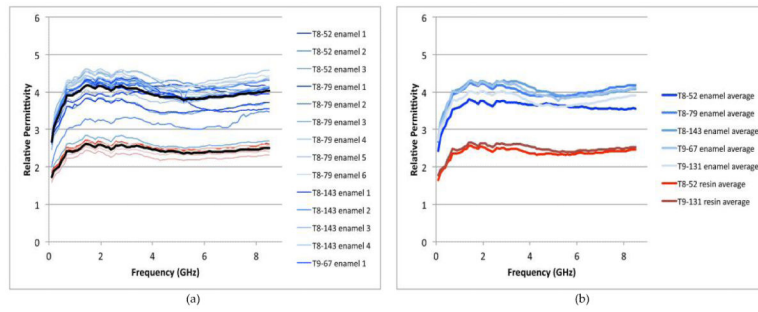


**FIGURE 6.**  
 (A) PLOT OF ALL SMALL PROBE MEASUREMENTS AS A FUNCTION OF FREQUENCY. THE BLUE LINES ARE THE ENAMEL MEASUREMENTS AND THE RED CORRESPOND TO THE RESIN ONES. THE HEAVIER BLACK LINES ARE THE AVERAGES FOR ALL ENAMEL AND ALL RESINS. (B) PLOT OF THE AVERAGE MEASUREMENTS FOR EACH TOOTH AND TYPE (ENAMEL OR RESIN) AS A FUNCTION OF FREQUENCY. THE BLUE LINES ARE THE ENAMEL MEASUREMENTS AND THE RED THE CORRESPONDING RESIN ONES.

Author Manuscript

Author Manuscript

Author Manuscript

Author Manuscript

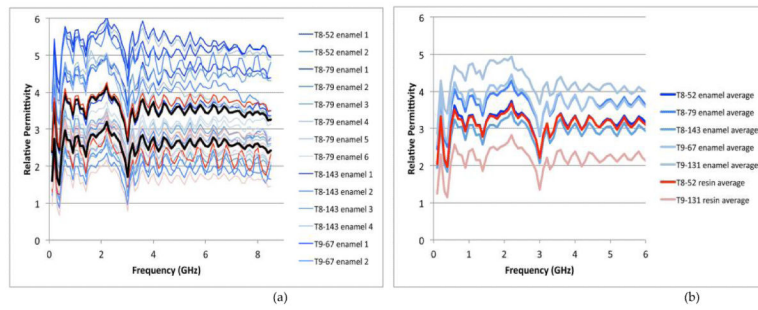


**FIGURE 7.**  
 (A) PLOT OF ALL LARGE PROBE MEASUREMENTS AS A FUNCTION OF FREQUENCY. THE BLUE LINES ARE THE ENAMEL MEASUREMENTS AND THE RED CORRESPOND TO THE RESIN ONES. THE HEAVIER BLACK LINES ARE THE AVERAGES FOR ALL ENAMEL AND ALL RESINS. (B) PLOT OF THE AVERAGE MEASUREMENTS FOR EACH TOOTH AND TYPE (ENAMEL OR RESIN) AS A FUNCTION OF FREQUENCY. THE BLUE LINES ARE THE ENAMEL MEASUREMENTS AND THE RED THE CORRESPONDING RESIN ONES.

Author Manuscript

Author Manuscript

Author Manuscript

Author Manuscript

TABLE 1 PROBE DIAMETERS AND THE ASSOCIATED PENETRATION DEPTHS FOR FOUR DIFFERENT DIAMETER DELFIN TECHNOLOGIES PROBES.

Model	Probe Diameter (mm)	Penetration Depth (mm)
L50	55	4.09
M25	33	2.74
S15	20	1.84
XS5	10	0.84

Author Manuscript

Author Manuscript

Author Manuscript

Author Manuscript